UNIVERSITY
OF TRENTO

DIPARTIMENTO DI INGEGNERIA E SCIENZA DELL'INFORMAZIONE

38123 Povo – Trento (Italy), Via Sommarive 14
http://www.disi.unitn.it

PATTERN SYNTHESIS IN TIME-MODULATED LINEAR ARRAYS THROUGH PULSE SHIFTING

L. Poli, P. Rocca, L. Manica, and A. Massa

January 2011

Technical Report # DISI-11-074

Pattern Synthesis in Time-Modulated Linear Arrays through Pulse Shifting

L. Poli, P. Rocca, L. Manica, and A. Massa, *Member, IEEE*

ELEDIA Research Group

Department of Information Engineering and Computer Science,

University of Trento, Via Sommarive 14, 38050 Trento - Italy

Tel. +39 0461 882057, Fax +39 0461 882093

E-mail: *andrea.massa@ing.unitn.it*,

{*lorenzo.poli, paolo.rocca, luca.manica*}*@disi.unitn.it*

Web-site: *http://www.eledia.ing.unitn.it*

Pattern Synthesis in Time-Modulated Linear Arrays through Pulse Shifting

L. Poli, P. Rocca, L. Manica, and A. Massa

Abstract

In this paper, an innovative approach for the synthesis of time-modulated linear array antennas is presented. The switch-on instants of the time-modulated elements are taken into account as additional degrees of freedom to optimize the array pattern. Towards this end, a technique based on a Particle Swarm Optimization is proposed to fully exploit the dependence of the sideband radiations on the shift of the time pulses. A set of representative results are reported to assess the effectiveness of the proposed approach as well as its flexibility.

Key words: Linear arrays, Time-Modulated Arrays, Pattern Synthesis.

1 Introduction

The use of time-modulated antenna arrays for the synthesis of patterns with low and ultra-low sidelobes has been first investigated by Kummer *et al.* in [1]. By exploiting the time as an additional degree of freedom for the synthesis [2], a set of RF switches has been used to enforce a time modulation on the element excitations [3][4]. The possibility of reconfiguring the array pattern by simply adjusting the on-off switching sequence identifies this strategy as a good candidate to deal with time-varying wireless scenarios. However, the generation of undesired harmonics [i.e., the so-called "sideband radiations" (SR)] represents a non-negligible drawback because of the loss of radiated energy. In order to properly address such an issue and improving the efficiency of the approach with respect to the results in [1], suitable evolutionary optimization algorithms have been recently considered [5]-[11]. In [5] and [6], the sideband level (SBL) has been significantly reduced through the optimization of the "static-mode" coefficients as well as of the durations of the time pulses by means of a Differential Evolution (DE) algorithm. A similar DE-based technique has been successively adopted in the synthesis of moving phase center antenna arrays for radar applications [7][10] to suppress the sideband radiations and to increase the passband of the receiver. Moreover, a Simulated Annealing (SA) technique has been used in [8] to minimize the sidelobe level (SLL) at the carrier frequency as well as the SBL of a time-modulated array with uniformly-excited elements. A different time schema has been successfully exploited in [11], where the modulation period has been quantized into shorter time steps and the on-off sequence optimized by means of a Genetic Algorithm (GA).
Although significant contributions in dealing with time modulation have been proposed, it should be also noticed that an implementation based on feeding networks with uniform distributions and the possibility of reconfiguring the beam pattern just modifying the on-off sequence of a set of RF switches have been only partially investigated and few applications envisaged. As a matter of fact, to the best of the authors' knowledge, the state-of-the-art literature is limited to the synthesis of compromise sum and difference patterns [12] and only recently a preliminary discussion on the features of the use of different switching schemes has been presented in [13]. In such a framework, this paper is aimed at analyzing and fully exploiting some issues previously only partially addressed in [13]. Starting from the mathematical proof that the SR is

a function of the "switch-on intervals" (i.e., the durations of the rectangular time pulses of the time modulation sequence), likewise the pattern shape at the fundamental frequency [1][5][8], but also of the switch-on instants (i.e., the time instants when the RF switches commute from open to short circuit), the optimization of the switch-on instants of the array elements is profitably performed for pattern synthesis purposes. Towards this end, two different synthesis problems will be addressed by acting on the switch-on instants. The first one is concerned with the minimization of the SBL, while generating a desired pattern at the carrier frequency. Notwithstanding the non-negligible advantage of generating whatever pattern at the working frequency, it is well known [14] that the power losses due to the unavoidable presence of the harmonic radiations still remains whether only the optimization of the switch-on instants of the time pulses (i.e., a pulse shifting in the period of the time sequence) is taken into account. Therefore, the reduction of the power losses caused by the SR is successively addressed by contemporaneously tuning during the synthesis process both the pulse durations and the switch-on instants.

The outline of the paper is as follows. In Section 2, the theory of time-modulated linear arrays is briefly summarized and some more details on the dependence of the radiated pattern on the switch-on instants are given. Section 3 is devoted to the numerical analysis. More specifically, a set of representative results concerned with the SBL minimization while synthesizing a desired pattern at the carrier frequency is shown in Sect. 3.1. Moreover, the minimization of the power losses is also performed (Section 3.2) still exploiting the effects of the pulse shift on the synthesized pattern to further point out the effectiveness and flexibility of the proposed methodology. Eventually (Sect. 4), some conclusions are drawn.

2 Mathematical Formulation

Let us consider a time-modulated linear array ($TMLA$) composed by N identical elements equally-spaced of d along the z axis. The spatial distribution of the array elements is supposed to be symmetric about the origin and the periodic on-off time sequences $U_n(t)$, $n = 0, ..., N-1$, which modulate the array element excitations, are obtained by means of on-off RF switches. The arising far-field radiation pattern can be expressed as follows [1]

$$F(\theta,t) = e_0(\theta)\, e^{j\omega_0 t} \sum_{n=0}^{N-1} \alpha_n U_n(t)\, e^{jknd\cos\theta} \tag{1}$$

where $e_0(\theta)$ and $\omega_0 = 2\pi f_0$ denote the element factor and the central angular frequency, respectively. Moreover, $k = \frac{2\pi}{\lambda_0}$ is the background wavenumber, $\mathbf{A} = \{\alpha_n,\, n = 0, ..., N-1\}$, is the set of static and complex array excitations, and θ indicates the angular position with respect to the array axis. The function $U_n(t)$ [Fig. 1] is assumed to have a period equal to T_p and it is mathematically described as

$$U_n(t) = \begin{cases} 1, & t'_n \le t \le t''_n \\ 0, & otherwise \end{cases} \tag{2}$$

where $0 \le t'_n \le t''_n \le T_p$. Moreover, the condition $T_p \gg T_0 = \frac{1}{f_0}$ is supposed to hold true [14]. Because of the periodicity of $U_n(t)$, its Fourier representation turns out to be

$$U_n(t) = \sum_{h=-\infty}^{\infty} u_{hn} e^{jh\omega_p t} \tag{3}$$

where the h-th Fourier coefficients, u_{hn}, is given by

$$u_{hn} = \frac{1}{T_p} \int_0^{T_p} U_n(t)\, e^{-jh\omega_p t} dt \tag{4}$$

$\omega_p = 2\pi f_p = \frac{2\pi}{T_p}$.

By considering isotropic radiators, [i.e., $e_0(\theta) = 1$] and without loss of generality of the arising conclusions, the radiated far-field pattern turns out to be [14]

$$F(\theta,t) = \sum_{h=-\infty}^{\infty} \left[\sum_{n=0}^{N-1} a_{hn} e^{jknd\cos\theta} \right] e^{j(h\omega_p + \omega_0)t} = \sum_{h=-\infty}^{\infty} F_h(\theta,t) \tag{5}$$

where $a_{hn} = \alpha_n u_{hn}$, $n = 0, ..., N-1$.

With reference to (5), the beam pattern at the carrier frequency f_0 depends on the 0-th order coefficients [1][5][8]

$$a_{0n} = \alpha_n u_{0n}\ ,\ n = 0, ...N-1 \tag{6}$$

where u_{0n} is the 0-th order Fourier coefficient [Eq. 4 - $h = 0$] equal to

$$u_{0n} = \frac{1}{T_p} \int_0^{T_p} U_n(t)\, dt = \tau_n \tag{7}$$

$\tau_n = \frac{(t''_n - t'_n)}{T_p}$ being the normalized n-th time pulse duration. It is worth noticing [Eq. (6)] that, when the values of the complex static coefficients, α_n, $n = 0, ..., N-1$ are fixed, the pattern

generated at the fundamental frequency ($h = 0$) is only function of the pulse durations τ_n, $n = 0, ..., N-1$. Accordingly, it is possible to synthesize a desired pattern, $\widehat{F}_0(\theta, t)$, different from the "static mode" (i.e., the mode generated by the static excitation set $\mathbf{A}$), by simply enforcing a suitable on-off time sequence to the static array excitations such that $\alpha_n \tau_n = \hat{a}_{0n}$ [(1)], $n = 0, ..., N-1$, $\hat{a}_{0n}$ being the n-th target excitation.

Unfortunately, "*the radiation patterns at the harmonic frequencies have significant components in the boresight direction*" [13]. In order to cope with such a drawback, unlike acting only on the pulse duration τ_n [8], a different approach must be adopted in order to reduce the SBL, as well. Towards this purpose, let us observe that the sideband radiation coefficients ($h \neq 0$)

$$a_{hn} = \frac{\alpha_n}{T_p}\left(\frac{e^{-jh\omega_p t'_n} - e^{-jh\omega_p t''_n}}{jh\omega_p}\right) \ , \ n = 0, ..., N-1, \tag{8}$$

can be also expressed, after simple mathematical manipulations, as follows

$$a_{hn} = \begin{cases} \alpha_n \tau_n sinc(\pi h \tau_n)\, e^{-j\pi h\left(\tau_n + 2\frac{t'_n}{T_p}\right)} & if\ 0 \leq \frac{t'_n}{T_p} \leq (1-\tau_n) \\ \frac{1}{\pi h}\left\{ sin\left[\pi h\left(1 - \frac{t'_n}{T_p}\right)\right] e^{-j\pi h\left(1+\frac{t'_n}{T_p}\right)} + \right. & \\ \left. sin\left[\pi h\left(\frac{t'_n}{T_p} + \tau_n - 1\right)\right] e^{-j\pi h\left(\frac{t'_n}{T_p}+\tau_n-1\right)} \right\} & if\ (1-\tau_n) < \frac{t'_n}{T_p} \leq 1 \end{cases} . \tag{9}$$

Such an expression points out that the coefficients related to the undesired harmonic radiation depend on the pulse durations τ_n, $n = 0, ..., N-1$, analogously to the fundamental frequency counterparts [Eq. (6)], but also on the switch-on time instants, t'_n, $n = 0, ..., N-1$. Thanks to this property, it is possible to spread the power associated to the SR as uniformly as possible over the whole visible angular space above the antenna (i.e., lowering the levels of the undesired harmonics along the boresight direction) by keeping the τ_n, $n = 0, ..., N-1$, values and optimizing the pulse shifts t'_n, $n = 1, ..., N$ [Fig. 1(*b*)]. Accordingly, a suitable strategy based on a Particle Swarm Optimizer (PSO) [15][16] is used to minimize the following cost function Ψ that quantifies the mismatch between the user-defined sideband level, SBL^{ref}, and the sideband levels, $SBL^{(h)} = SBL(\omega_0 + h\omega_p)$, $h = 1, ..., \infty$, of the synthesized pattern

$$\Psi(\mathbf{t}')|_{\mathbf{T}=\widehat{\mathbf{T}}} \ = \ \sum_{h=1}^{\infty}\left\{ H\left[SBL^{ref} - SBL^{(h)}(\mathbf{t}')\right] \left|\Delta_{SBL}^{(h)}(\mathbf{t}')\right|^2 \right\} \tag{10}$$

[(1)] Under the condition that $arg(\alpha_n) = arg(\hat{a}_{0n})$ since τ_n, $n = 0, ..., N-1$ are real-valued quantities.

where $\Delta_{SBL}^{(h)}(\mathbf{t}') = \frac{SBL^{ref} - SBL^{(h)}(\mathbf{t}')}{SBL^{ref}}$, $\mathbf{t}' = \{t'_n;\ n = 0, ..., N-1\}$, $\mathbf{T} = \{\tau_n;\ n = 0, ..., N-1\}$, and $H(\cdot)$ stands for the Heaviside step function.

On the other hand, when the constraint of exactly matching the desired pattern at f_0, $\widehat{F}_0(\theta, t)$, is relaxed [e.g., the synthesized pattern $F(\theta, t)$ is required at f_0 to fit the desired one in terms of SLL and main lobe beamwidth BW], it is still possible to profitably exploit the "pulse shifting" paradigm by tuning the pulse durations, τ_n, $n = 0, ..., N-1$, as well, to reduce the power losses of the SR together with the corresponding SBL. Towards this end, the optimization is reformulated by defining the following matching function composed by three terms

$$\begin{aligned}\Psi(\mathbf{t}', \mathbf{T}) &= \psi_{SLL}\left\{H\left[\Delta_{SLL}(\mathbf{T})\right]\left|\Delta_{SLL}(\mathbf{T})\right|^2\right\} + \psi_{BW}\left\{H\left[\Delta_{BW}(\mathbf{T})\right]\left|\Delta_{BW}(\mathbf{T})\right|^2\right\} + \\ &+ \psi_{SBL}\sum_{h=1}^{\infty}\left\{H\left[\Delta_{SBL}^{(h)}(\mathbf{t}', \mathbf{T})\right]\left|\Delta_{SBL}^{(h)}(\mathbf{t}', \mathbf{T})\right|^2\right\}\end{aligned} \tag{11}$$

where $\Delta_{SLL}(\mathbf{T}) = \frac{SLL^{ref} - SLL(\mathbf{T})}{SLL^{ref}}$ and $\Delta_{BW}(\mathbf{T}) = \frac{BW^{ref} - BW(\mathbf{T})}{BW^{ref}}$. Moreover, ψ_{SLL}, ψ_{BW}, ψ_{SBL} are real-valued weighting coefficients.

3 Numerical Results

In this section, a set of representative results are reported to point out the effectiveness and flexibility of the proposed methodology. The numerical validation is subdivided into two parts. The first one (Sect. 3.1) is aimed at illustrating the efficiency of the pulse-shift technique in minimizing the SBL. Towards this end and for comparative purposes, the illustrative test cases have been chosen among those already considered in the published literature. In the second part (Sect. 3.2), the examples under analysis are concerned with both the SBL minimization and the SR power reduction.

3.1 SBL Reduction with Fixed Power Losses

With reference to an array of $N = 16$ $\frac{\lambda}{2}$-spaced elements, let us consider the problem dealt with in [13] and concerned with the synthesis at the carrier frequency of a Chebyshev pattern [17] with $SLL = -30\,dB$ [Fig. 2(*a*)] starting from the "static mode" (i.e., the beam pattern generated by the uniform excitation set $\mathbf{A}^{(I)} = \{\alpha_n = 1;\ n = 0, ..., N-1\}$). Figure 3(*a*) gives

a pictorial representation of the switching sequence synthesized in [13] by acting on $\mathbf{T}$. As expected [Eq. (6)], the durations of the time pulses are equal to the values of the samples of the normalized Chebyshev distribution [17] (i.e., $\mathbf{T} = \mathbf{T}_{DC}$).

However, even though the reference pattern at f_0 is exactly matched, the harmonic content along the boresight direction is non-negligible [Fig. 2(*b*)]. In order to cope with this drawback, the pulse-shifting technique has been then used as described in Sect. 2. Accordingly, the set $\mathbf{t}'$ (being $\widehat{\mathbf{T}} = \mathbf{T}_{DC}$) has been optimized by choosing $SBL^{ref} = -25\,dB$ and minimizing the cost function in (10) with $h = 1$ [(2)] since the power losses associated to higher harmonics decrease faster [14]. Towards this purpose, a PSO with $I = 10$ particles and a standard setting [18] of the control parameters (i.e., $w = 0.4$ and $C_1 = C_2 = 2$; w, C_1, and C_2 being the inertial weight and the cognitive/social acceleration terms, respectively) has been used.

The PSO-optimized pulse sequence is shown in Fig. 3(*b*). Moreover, the radiated patterns are displayed in Fig. 4 and compared with those from [13] up to the second harmonic mode. As it can be observed, the SBL at $h = 1$ is equal to $SBL^{(1)}_{PSO} = -19.50\,dB$ and its value results more than $7\,dB$ below that in [13] (i.e., $SBL^{(1)}_{DC} = -12.40\,dB$). Moreover, although the harmonic frequency $h = 2$ is not directly involved in the optimization process, it turns out that $SBL^{(2)}_{PSO} = -21.70\,dB$ vs. $SBL^{(2)}_{DC} = -18.30\,dB$. For completeness, the comparison in terms of maximum SBL of the harmonic patterns is extended to higher orders (Fig. 5). It is worth noticing that over 30 harmonics, 29 PSO-synthesized patterns have SBLs lower than those generated by the pulse configuration $\mathbf{T}_{DC}$ in [Fig. 3(*a*)] since only the case $h = 16$ presents a SBL worse of almost $1\,dB$. Such a result further confirms the intrinsic "robustness" of the pulse shifting methodology.

As regards the energy wasted in the SR and independent from pulse shifting, the loss of energy amounts to the 25.2% of the total input power [14] and the SBLs results greater than the side lobes of the desired Dolph-Chebyshev pattern ($SLL = -30\,dB$) at the carrier frequency. As a matter of fact, since there is a trade-off (for a given antenna layout) between the desired SLL and beamwidth at $h = 0$ and the SR, the SBL values can be be higher than the SLL as in this case.

[(2)] It should be pointed out that more terms (i.e., $h > 1$) might be considered in (10) to directly control the SBLs of other undesired harmonic terms.

As far as the computational issues are concerned, the behavior of the optimal value of Ψ (i.e., $\Psi^{opt} = min_k \left\{ min_i \left[\Psi \left(\mathbf{t'}_{i_k} \right)|_{\mathbf{T}=\mathbf{T}_{DC}} \right] \right\}$, i_k being the index of the i-th particle of the swarm at the k-th iteration of the minimization process) and the corresponding SBL values are reported in Fig. 6. As regards the CPU-time, it amounts to $74.16\,[sec]$ to complete the whole number of $K = 1000$ PSO iterations on a $3\,GHz$ PC with $1\,GB$ of RAM, $6.6 \times 10^{-3}\,[sec]$ being the time needed for a cost function evaluation.

The second experiment of this section refers to a scenario previously addressed in [8], where an array of $N = 30$ elements spaced by $d = 0.7\lambda$ has been considered. In [8], by exploiting a SA-based strategy, the set $\mathbf{T}$ has been optimized (i.e., $\mathbf{T} = \mathbf{T}_{SA}$) by minimizing a suitable cost function [Eq. (5) - [8]] devoted to set the following constraints on the generated beam pattern: $SLL < -20\,dB$ and $SBL^{(h)} < -30\,dB$, $|h| = 1, 2$. Likewise the previous example, in order to prove that keeping the same time-duration set $\mathbf{T}_{SA}$ (i.e., the same pattern at $h = 0$), it is possible to further lower the SBL by properly programming the switch-on instants of the RF switches, the proposed PSO-based algorithm has been applied.

The original [8] and the PSO-optimized time sequence are reported in Fig. 7(*a*) and Fig. 7(*b*), respectively. Moreover, Figure 8 shows the plots of the radiation patterns synthesized with the SA [8] and by means of the PSO algorithm at $|h| = 1$ and at the fundamental frequency ($h = 0$). As it can be observed, the level of the sideband radiation in correspondence with the first harmonic mode turns out to be $SBL_{SA}^{(1)} = -30.05\,dB$ while $SBL_{PSO}^{(1)} = -32.90\,dB$ with an improvement of about $3\,dB$ despite the reduced number of time modulated elements ($\frac{M}{N} < \frac{1}{3}$, $M = 9$ being the number of time-modulated elements). Furthermore, it is noteworthy that, thanks to the optimization of $\mathbf{t'}$, it also results $SBL_{PSO}^{(h)} < SBL_{SA}^{(h)}$, $h > 1$ [Fig. 9]. Concerning the SR, the amount of power losses turns out to be equal to 3.89%.

For completeness, the behavior of Ψ^{opt} and the arising $SBL^{(1)}$ value versus the iteration index k are shown in Fig. 10.

3.2 Joint SBL Minimization and SR Power Reduction

In order to assess the effectiveness of the pulse shifting technique also in dealing with the SR power reduction, let us consider the same benchmark of the first example in Sect. 3.1,

but now optimizing the pulse durations, as well. Towards this aim, the cost function (11) is adopted and the reference thresholds are set to $SLL^{ref} = -30\,dB$ and $BW^{ref} = 3.95^o$ to obtain a pattern with the same features of that afforded by the Chebyshev coefficients, by keeping $SBL^{ref} = -25\,dB$.

Figure 11 shows the pulse sequence synthesized by the PSO-based method when a swarm of $I = 20$ particles has been run for $K = 1000$ iterations. For comparison purposes, the normalized powers related to f_0 and to the sideband radiations are analyzed and Figure 12 shows the results obtained when acting on $\mathbf{T}$ [13] and also on $\mathbf{t}'$. As expected, there is a reduction of the losses due to the SR and an increasing of the radiation at f_0 when applying the pulse shifting. It is worthwhile to point out that such an enhancement of the performance is yielded without increasing the architectural complexity of the system with uniform excitations. For completeness, the patterns synthesized at the carrier frequency and when $h = 1, 2$ are shown in Fig. 13 and compared with those from the time-modulation scheme in Fig. 3(*a*).

As regards the computational costs, the computational burden grows since the number of unknowns double with respect to the case in Sect. 3.1 and the solution space of the admissible solutions significantly enlarges. Moreover, the CPU-time necessary to compute the cost function value (11) of each particle is about twice that when only $\mathbf{t}'$ was optimized (Sect. 3.1). Consequently, the total CPU-time required to sample the solution space with a swarm of $I = 20$ particles amounts to $262.01\,[sec]$, $1.3 \times 10^{-2}\,[sec]$ being the time-cost of a single evaluation of $\Psi\left(\mathbf{t}', \mathbf{T}\right)$.

Finally, Figure 14 gives some indications on the behaviors of the three terms of the cost function as well as of Ψ^{opt} throughout the iterative optimization process.

4 Conclusions

In this paper, an innovative approach for the synthesis of time-modulated linear arrays has been proposed. The method considers the on instants of the time pulses as a suitable and further degree of freedom in the synthesis process. Starting from the basic principles of the pulse shifting strategy, mathematically formulated according to the theory of time-modulated arrays, the synthesis problem has been recast as the optimization of a proper cost function modelling

the mismatch between the actual pattern features and the desired ones. Both SBL reduction and SR minimization issues have been addressed and the minimization of the corresponding cost function has been carried out by means of a PSO-based algorithm. A set of representative results has been reported and discussed in order to assess the potentialities of the proposed approach. The pulse-shift methodology has demonstrated to work effectively when compared to other techniques in dealing with examples usually considered in the state-of-the-art literature.

Acknowledgments

The authors would like to thank Prof. Franceschetti for inspiring this work and Prof. Ares for introducing them the basic concepts of the time modulation for the synthesis of array antennas.

References

[1] Kummer, W. H., Villeneuve, A. T., Fong, T. S., and Terrio, F. G.: 'Ultra-low sidelobes from time-modulated arrays', *IEEE Trans. Antennas Propag.*, 1963, 11, (6), pp. 633-639.

[2] Shanks, H. E., and Bickmore, R. W.: 'Four-dimensional electromagnetic radiators', *Canad. J. Phys.*, 1959, 37, pp. 263-275.

[3] Weeks, W. L.: 'Antenna Engineering' (New York: McGraw-Hill, 1968).

[4] Bickmore, R. W.: 'Time versus space in antenna theory' in Hansen, R. C.: 'Microwave Scanning Antennas', (Ed. Los Altos, CA: Peninsula, 1985), vol. III, ch. 4.

[5] Yang, S., Gan, Y. B., and Qing, A.: 'Sideband suppression in time-modulated linear arrays by the differential evolution algorithm', *IEEE Antennas Wireless Propag. Lett.*, 2002, 1, pp. 173-175.

[6] Yang, S., Gan, Y. B., and Tan, P. K.: 'A new technique for power-pattern synthesis in time-modulated linear arrays', *IEEE Antennas Wireless Propag. Lett.*, 2003, 2, pp. 285-287.

[7] Yang, S., Gan, Y. B., and Qing, A.: 'Moving phase center antenna arrays with optimized static excitations', *Microw. Opt. Technol. Lett.*, 2003, 38, pp. 83-85.

[8] Fondevila, J., Brégains, J. C., Ares, F. , and Moreno, E.: 'Optimizing uniformly excited linear arrays through time modulation', *IEEE Antennas Wireless Propag. Lett.*, 2004, 3, pp. 298-301.

[9] Yang, S., Gan, Y. B., and Tan, P. K.: 'Comparative study of low sidelobe time modulated linear arrays with different time schemes', *JEMWA*, 2004, 18, (11), pp. 1443-1458.

[10] Yang, S., Gan, Y. B., and Tan, P. K.: 'Linear antenna arrays with bidirectional phase center motion', *IEEE Trans. Antennas Propag.*, 2005, 53, (5), pp. 2337-2339.

[11] Yang, S., Gan, Y. B., Qing, A., and Tan, P. K.: 'Design of a uniform amplitude time modulated linear array with optimized time sequences', *IEEE Trans. Antennas Propag.*, 2005, 53, (7), pp. 2337-2339.

[12] Fondevila, J., Brégains, J. C., Ares, F., and Moreno, E.: 'Application of time modulation in the synthesis of sum and difference patterns by using linear arrays', *Microw. Opt. Technol. Lett.*, 2006, 48, pp. 829-832.

[13] Tennant A., and Chambers, B.: 'Control of the harmonic radiation patterns of time-modulated antenna arrays', *Proc. 2008 IEEE AP-S International Symp.*, S. Diego, California, USA, July 5-12, 2008.

[14] Brégains, J. C., Fondevila, J., Franceschetti, G., and Ares, F.: 'Signal radiation and power losses of time-modulated arrays', *IEEE Trans. Antennas Propag.*, 2008, 56, (6), pp. 1799-1804.

[15] Kennedy, J., Eberhart, R. C., and Shi, Y.: 'Swarm Intelligence' (San Francisco, CA: Morgan Kaufmann, 2001).

[16] Robinson, J., and Rahmat-Samii, Y., 'Particle swarm optimization in electromagnetics', *IEEE Trans. Antennas Propag.*, 2004, 52, (2), pp. 397-407.

[17] Dolph, C. L.: 'A current distribution for broadside arrays which optimizes the relationship between beam width and sidelobe level', *Proc. IRE*, 1946, 34, pp. 335-348.

[18] Donelli, M., Franceschini, G., Martini, A., and Massa, A.: 'An integrated multiscaling strategy based on a particle swarm algorithm for inverse scattering problems', *IEEE Trans. Geosci. Remote Sens.*, 2006, 44, (2), pp. 298-312.

FIGURE CAPTIONS

- **Figure 1.** Time pulse when (*a*) $0 \leq \frac{t'_n}{T_p} \leq (1-\tau_n)$ and (*b*) $(1-\tau_n) \leq \frac{t'_n}{T_p} \leq 1$.

- **Figure 2.** *Pulse Duration Optimization* [13] ($N = 16$, $d = 0.5\lambda$) - (*a*) Static and reference power patterns; (*b*) Power patterns generated at f_0 ($h = 0$) and in correspondence with the harmonic terms $h = 1, 2$.

- **Figure 3.** *Pulse Shift Optimization* ($N = 16$, $d = 0.5\lambda$) - Element on-off time sequence: (*a*) original [13] and (*b*) optimized with the PSO-based approach.

- **Figure 4.** *Pulse Shift Optimization* ($N = 16$, $d = 0.5\lambda$) - Original [13] and PSO-optimized power patterns at $h = 0, 1, 2$.

- **Figure 5.** *Pulse Shift Optimization* ($N = 16$, $d = 0.5\lambda$) - Behavior of the $SBL^{(h)}$ when $h \in [0,\ 30]$. Original [13] and PSO optimized values.

- **Figure 6.** *Pulse Shift Optimization* ($N = 16$, $d = 0.5\lambda$) - Behaviors of the optimal value of the cost function, Ψ^{opt}, and of $SBL^{(1)}$ versus the iteration index k.

- **Figure 7.** *Pulse Shift Optimization* ($N = 30$, $d = 0.7\lambda$) - Element on-off time sequence: (*a*) original [8] and (*b*) optimized with the PSO-based approach.

- **Figure 8.** *Pulse Shift Optimization* ($N = 30$, $d = 0.7\lambda$) - Power patterns at f_0 ($h = 0$) and when $h = 1$: original [8] and PSO-optimized plots.

- **Figure 9.** *Pulse Shift Optimization* ($N = 30$, $d = 0.7\lambda$) - Behavior of the $SBL^{(h)}$ when $h \in [0,\ 30]$. Original [8] and PSO optimized values.

- **Figure 10.** *Pulse Shift Optimization* ($N = 30$, $d = 0.7\lambda$) - Behaviors of the optimal value of the cost function, Ψ^{opt}, and of $SBL^{(1)}$ versus the iteration index k.

- **Figure 11.** *Joint Optimization of Pulse Shifts and Durations* ($N = 16$, $d = 0.5\lambda$) - PSO-optimized element on-time sequence.

- **Figure 12.** *Joint Optimization of Pulse Shifts and Durations* ($N = 16$, $d = 0.5\lambda$) - Normalized powers associated to f_0 ($h = 0$) and to the sideband radiations ($h \neq 0$) for pulse duration optimization [13] and PSO-based shift-duration pulse optimization.

- **Figure 13.** *Joint Optimization of Pulse Shifts and Durations* ($N = 16$, $d = 0.5\lambda$) - Power patterns at $h = 0, 1, 2$: PSO-based $(\mathbf{t}')$ and $(\mathbf{t}', \mathbf{T})$ optimizations.

- **Figure 14.** *Joint Optimization of Pulse Shifts and Durations* ($N = 16$, $d = 0.5\lambda$) - Behaviors of the cost function terms during the iterative PSO-based minimization.

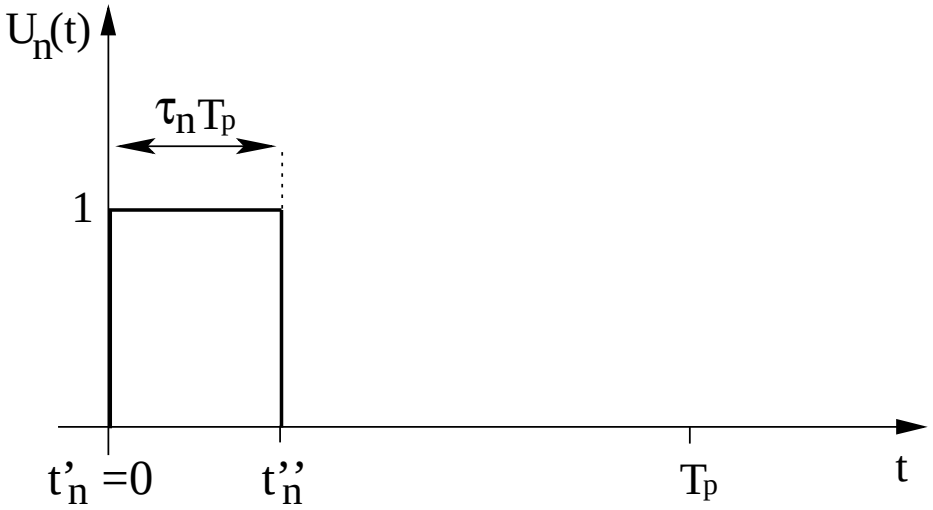

(a)

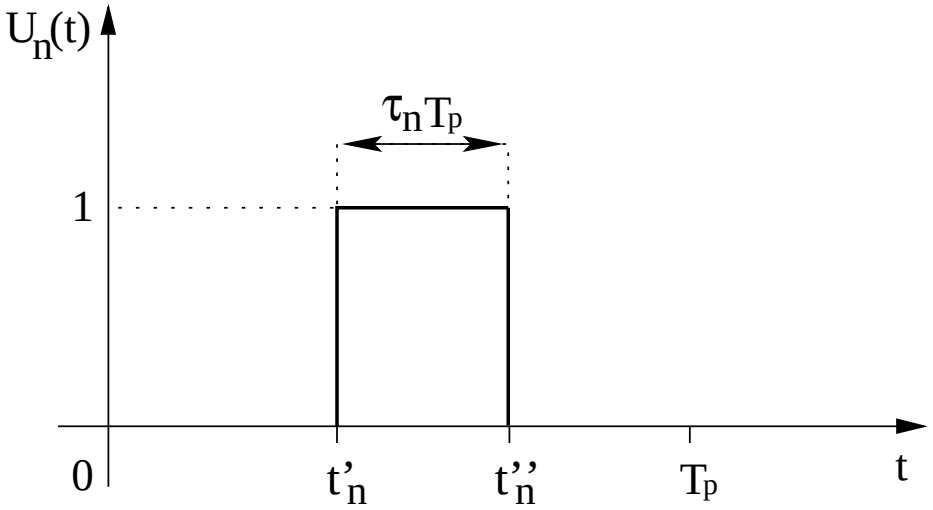

(b)

Fig. 1 - L. Poli *et al.*, "Pattern synthesis in time-modulated linear arrays ..."

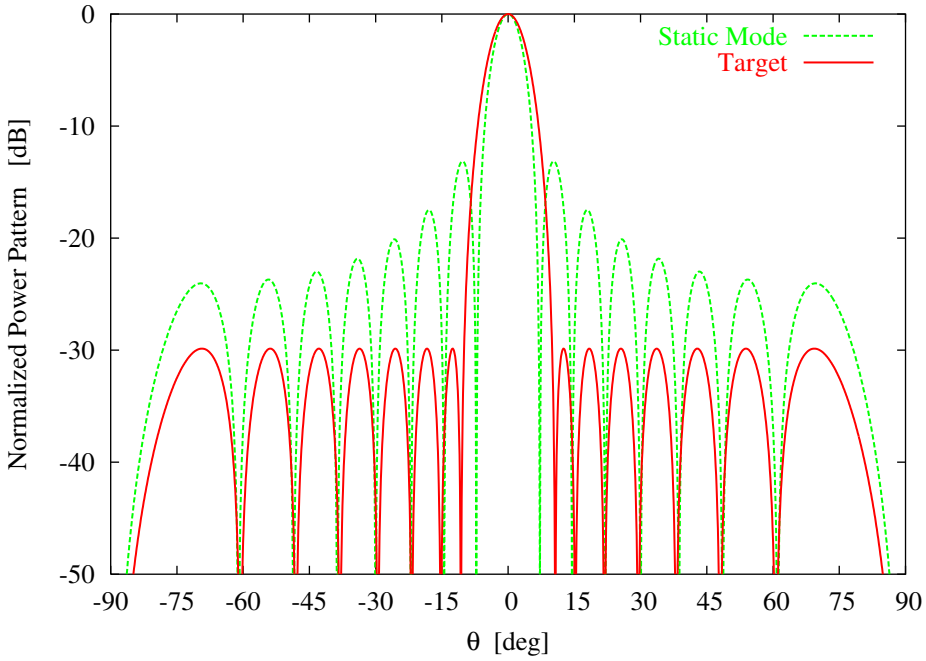

(a)

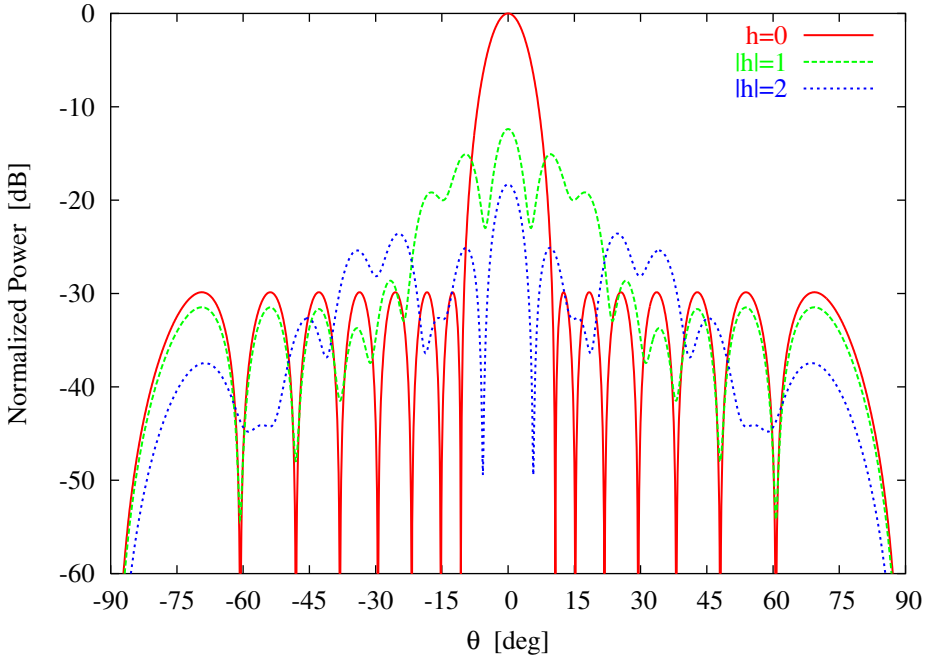

(b)

Fig. 2 - L. Poli *et al.*, "Pattern synthesis in time-modulated linear arrays ..."

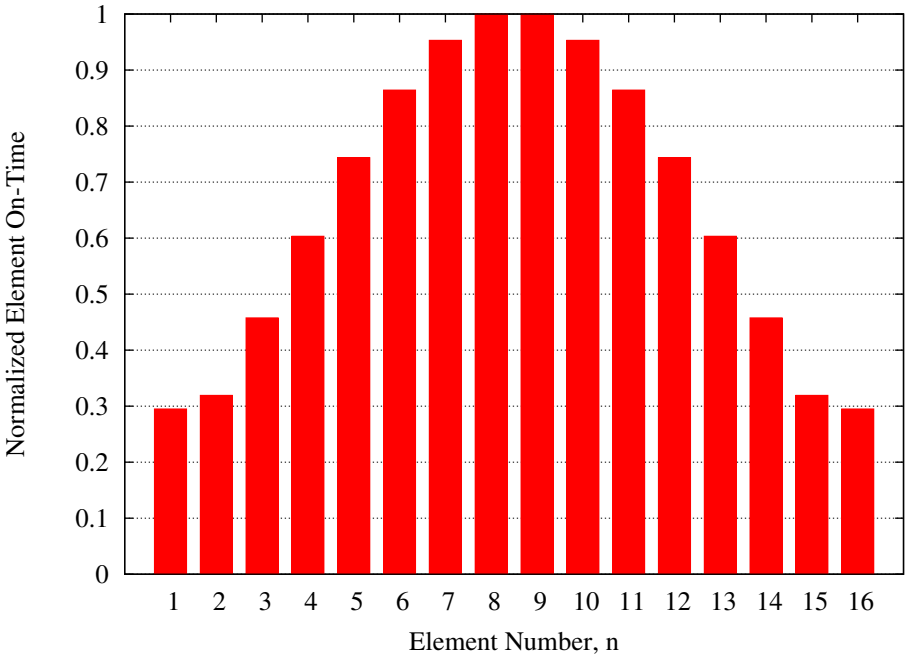

(a)

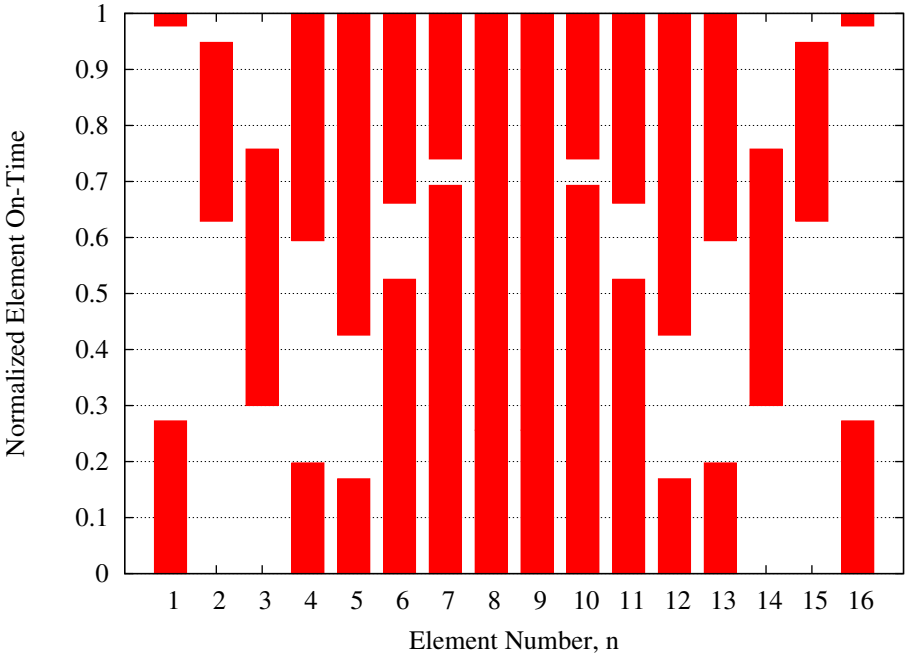

(b)

Fig. 3 - L. Poli *et al.*, "Pattern synthesis in time-modulated linear arrays ..."

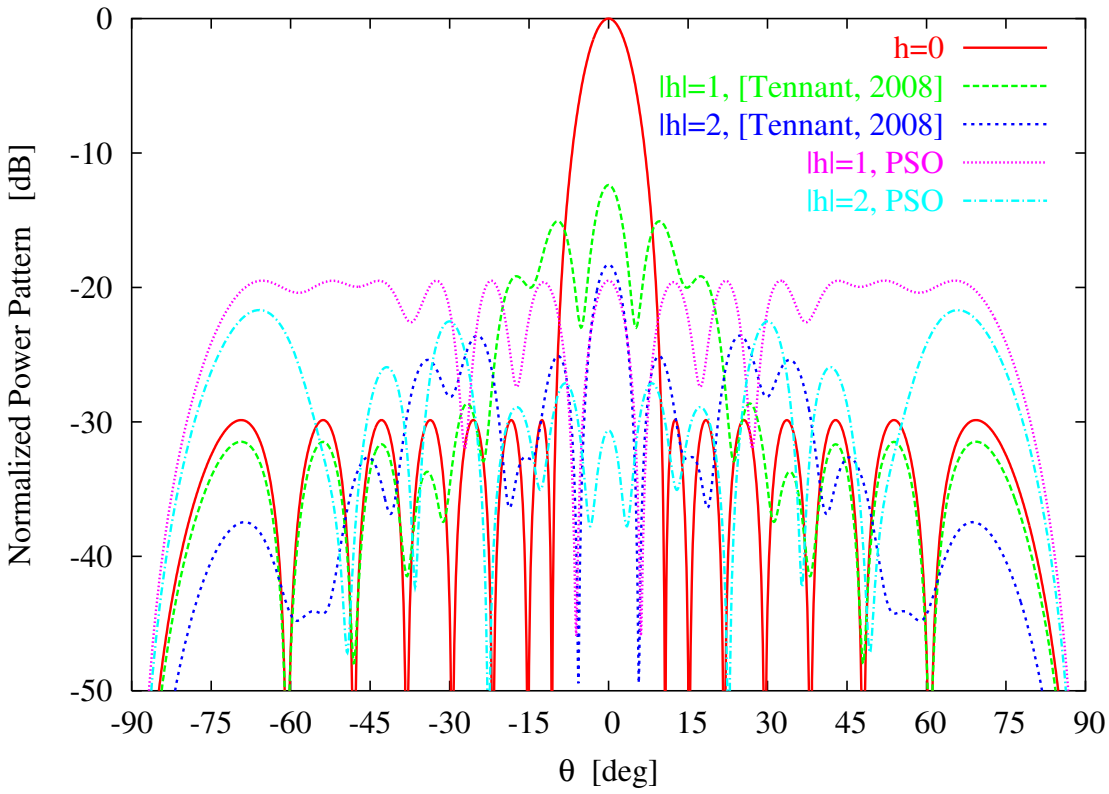

Fig. 4 - L. Poli *et al.*, "Pattern synthesis in time-modulated linear arrays ..."

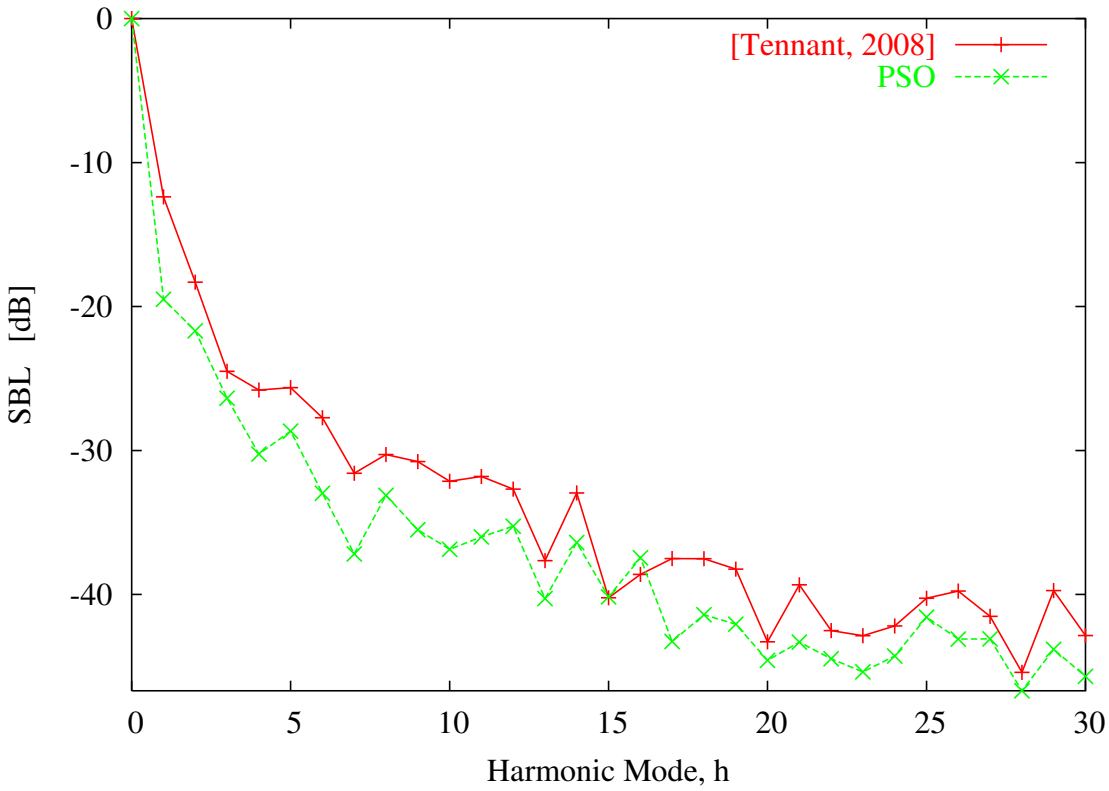

Fig. 5 - L. Poli *et al.*, "Pattern synthesis in time-modulated linear arrays ..."

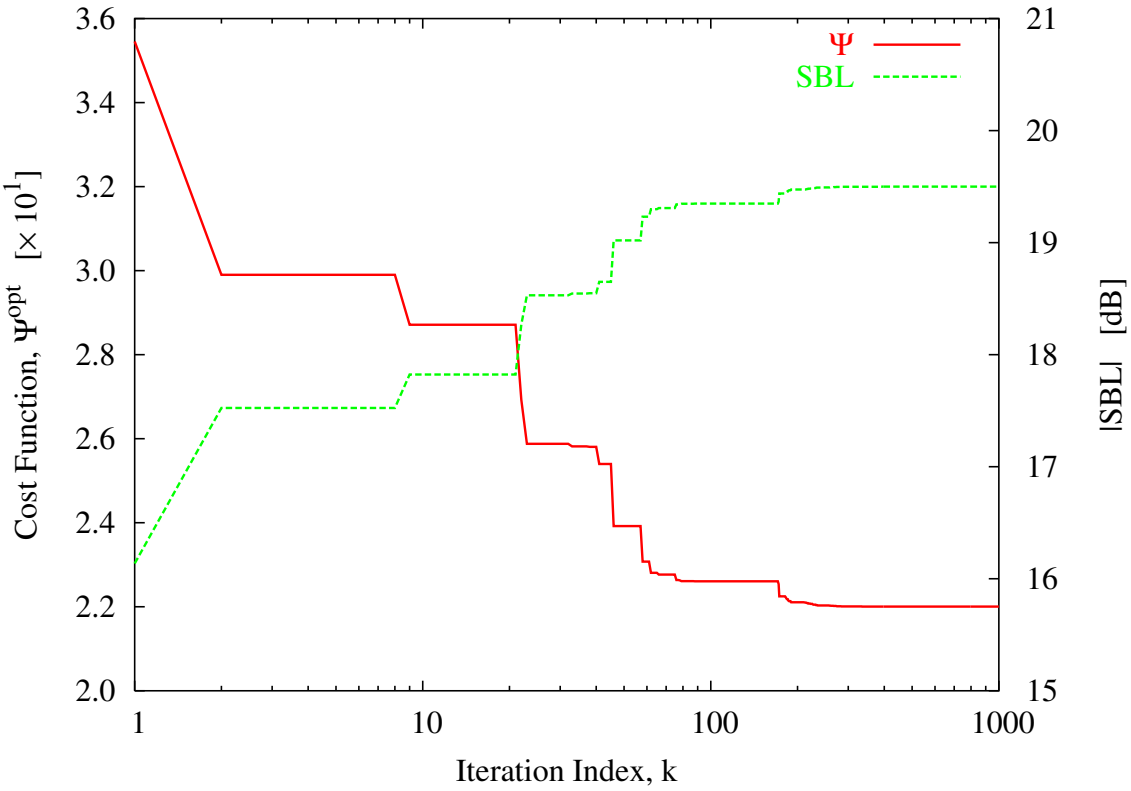

Fig. 6 - L. Poli *et al.,* "Pattern synthesis in time-modulated linear arrays ..."

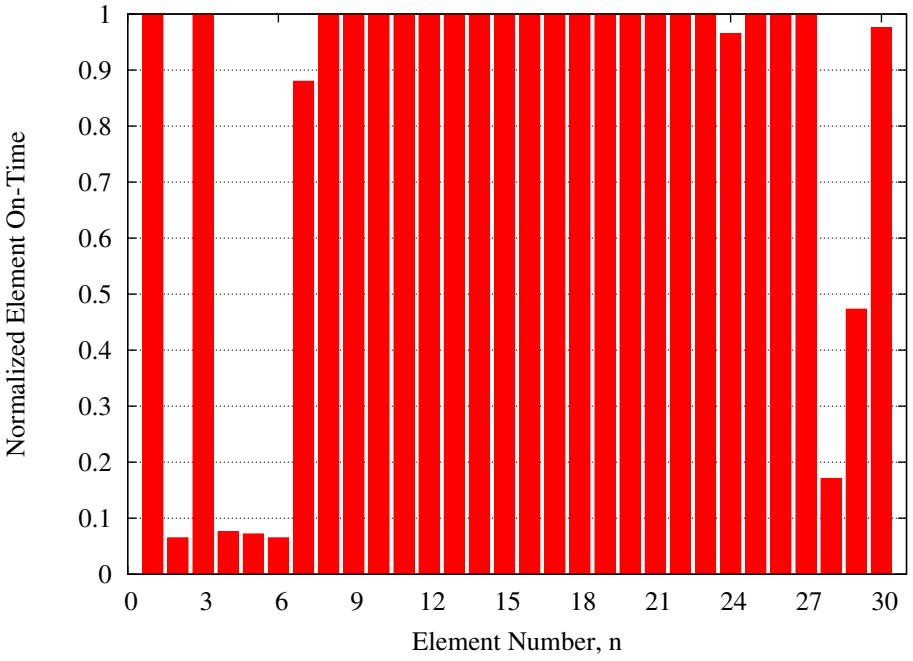

(a)

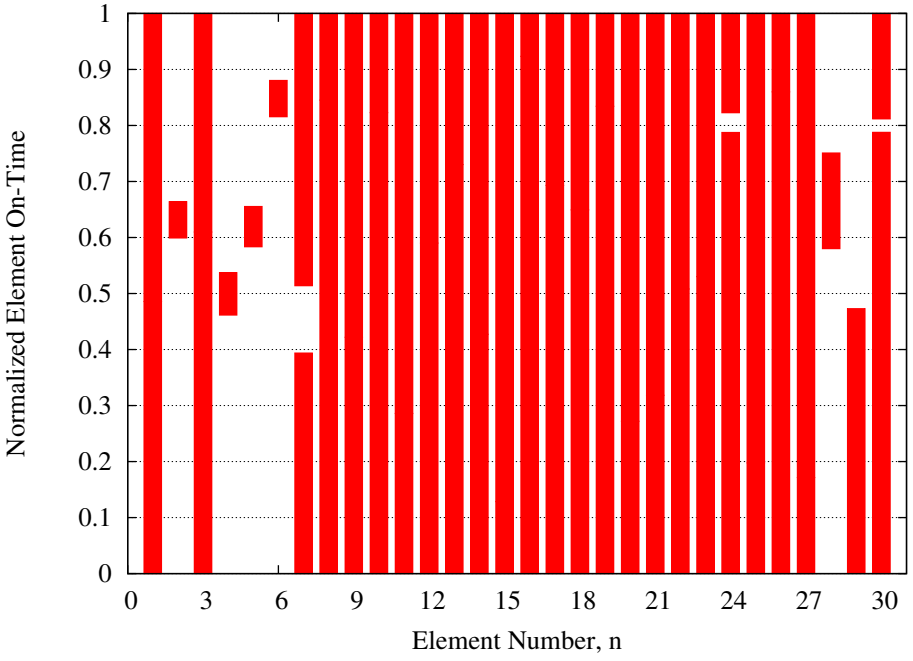

(b)

Fig. 7 - L. Poli *et al.*, "Pattern synthesis in time-modulated linear arrays ..."

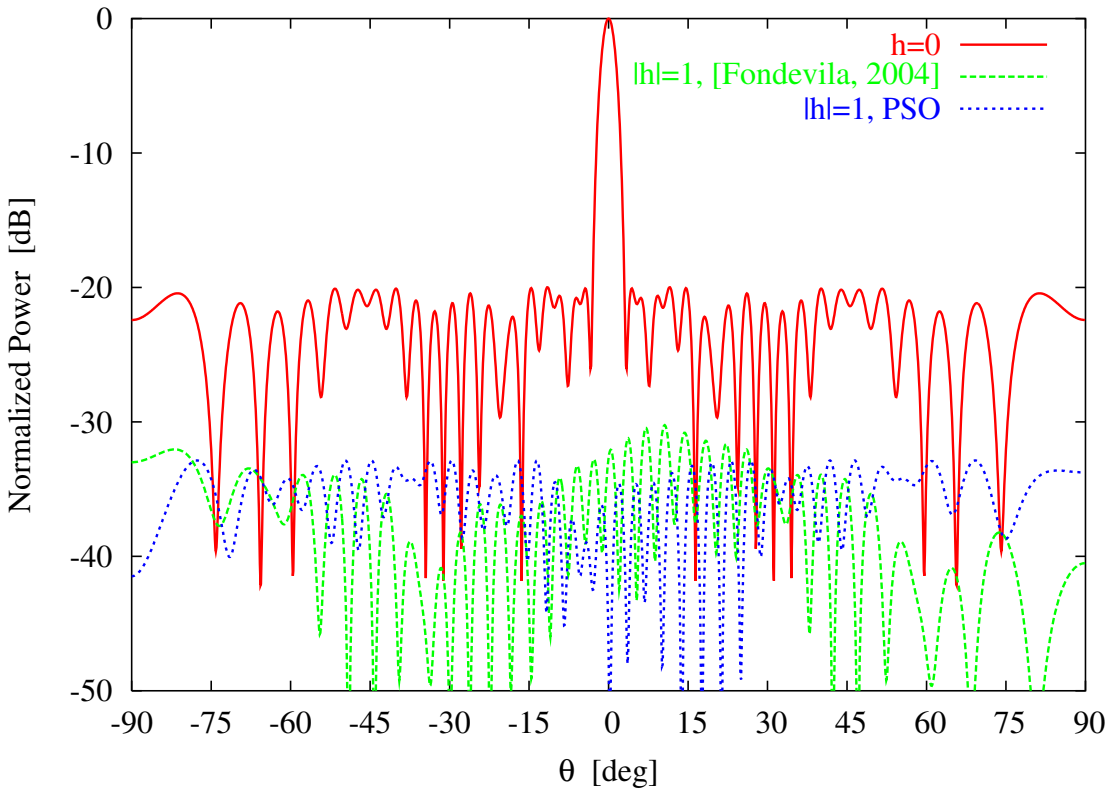

Fig. 8 - L. Poli *et al.*, "Pattern synthesis in time-modulated linear arrays ..."

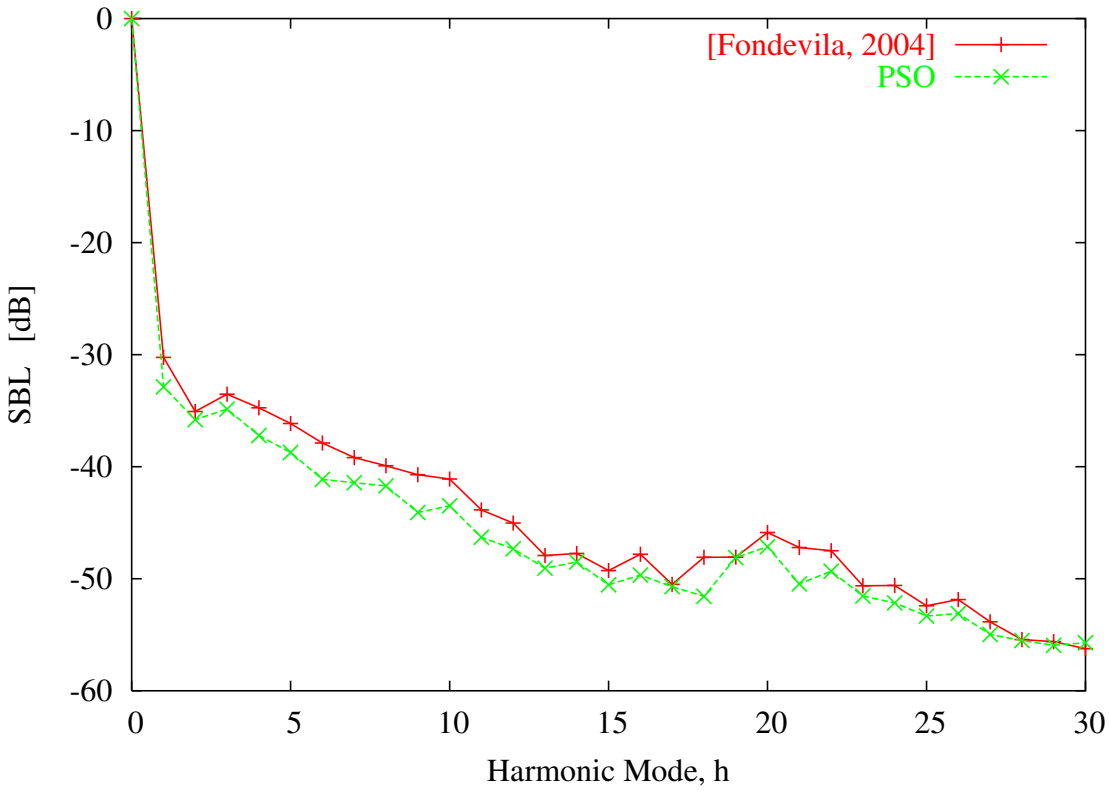

Fig. 9 - L. Poli *et al.*, "Pattern synthesis in time-modulated linear arrays ..."

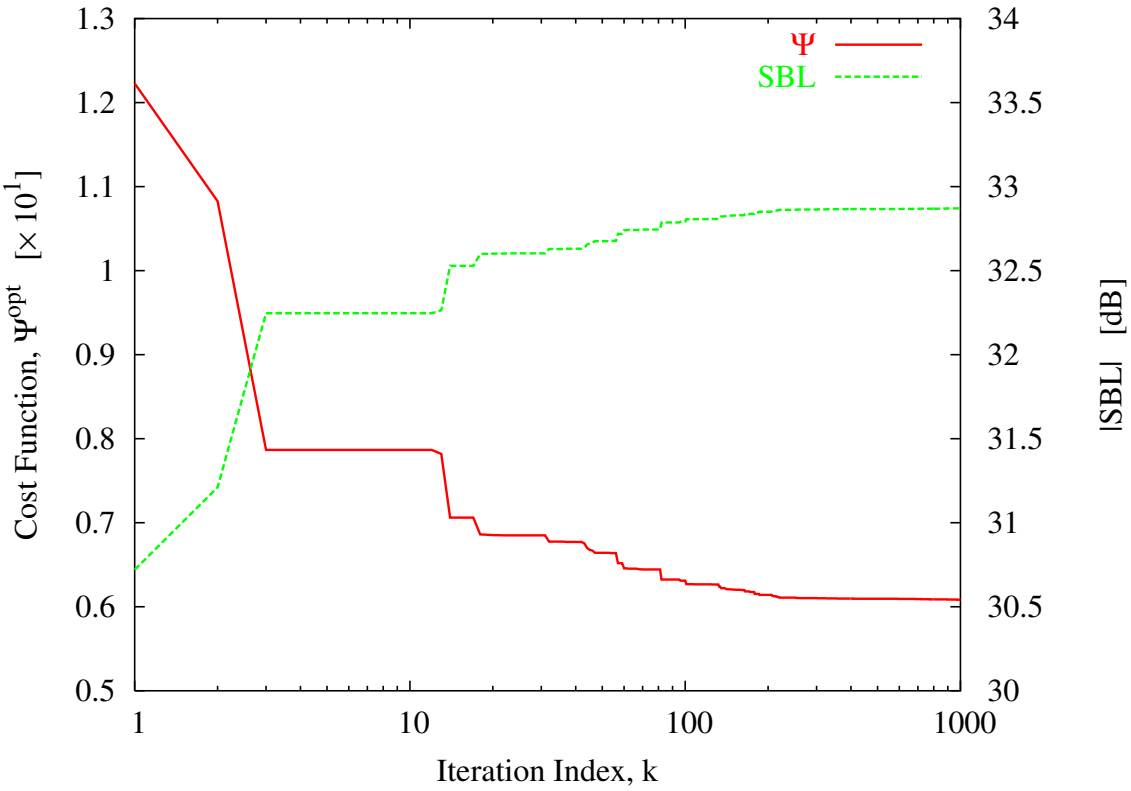

Fig. 10 - L. Poli *et al.*, "Pattern synthesis in time-modulated linear arrays ..."

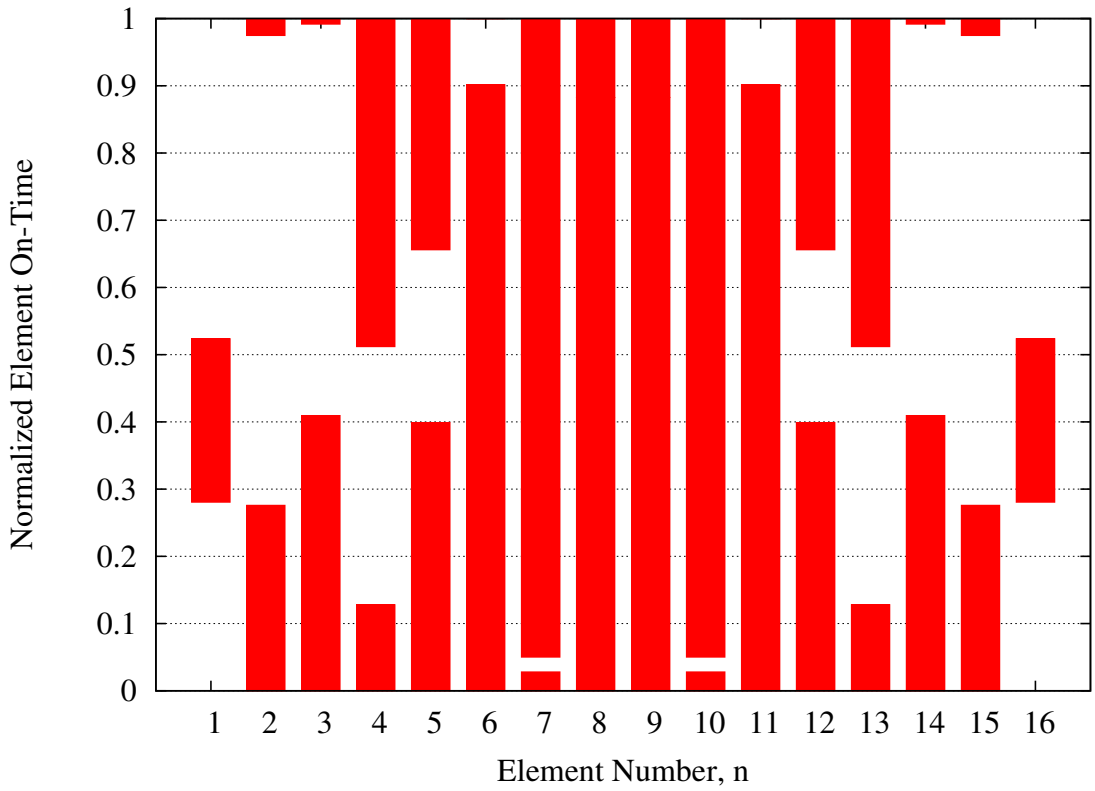

Fig. 11 - L. Poli *et al.*, "Pattern synthesis in time-modulated linear arrays ..."

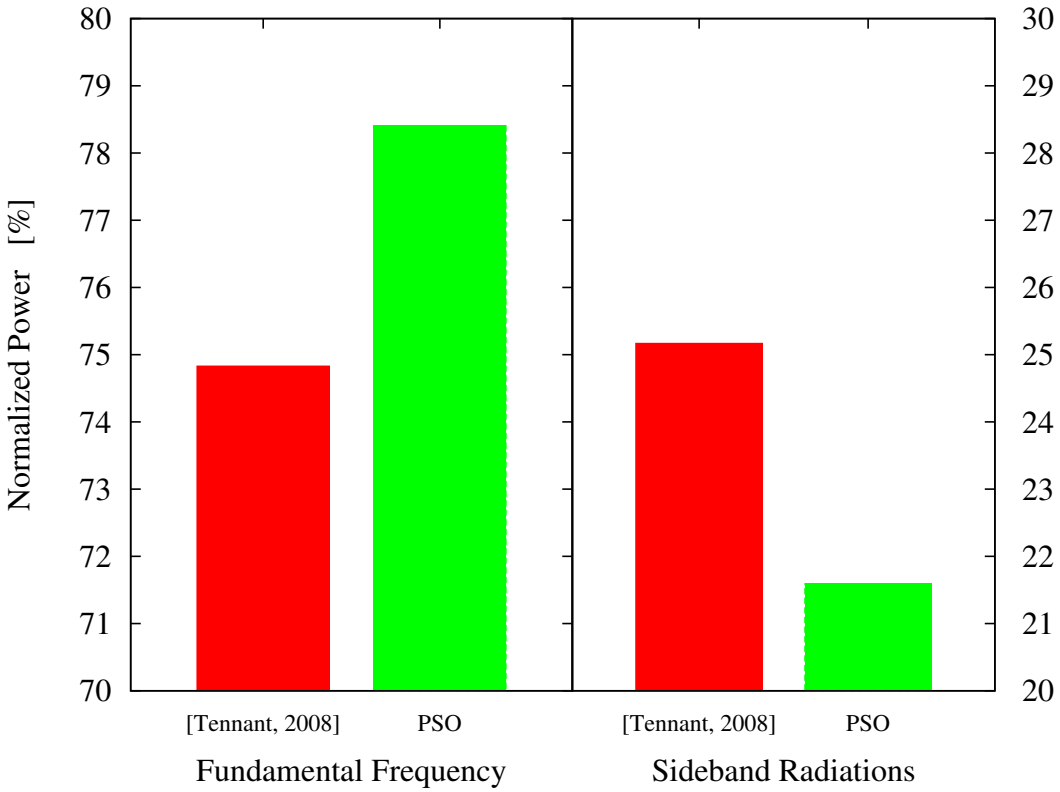

Fig. 12 - L. Poli *et al.*, "Pattern synthesis in time-modulated linear arrays ..."

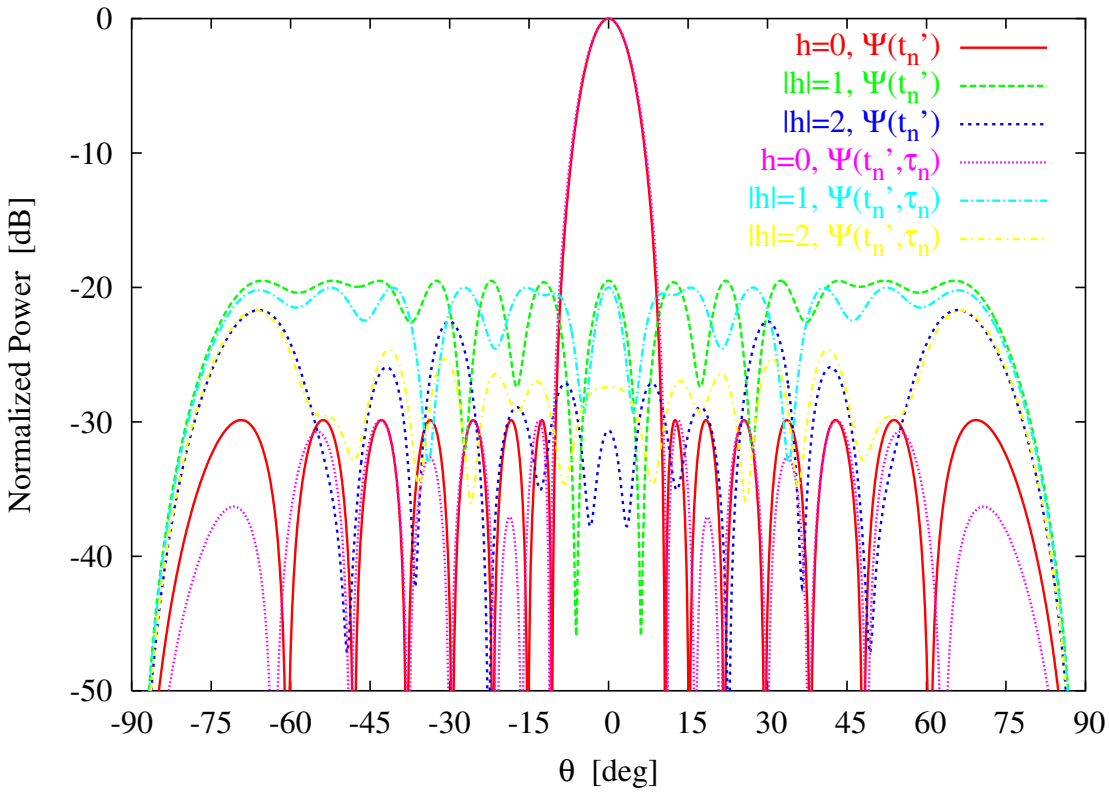

Fig. 13 - L. Poli *et al.*, "Pattern synthesis in time-modulated linear arrays ..."

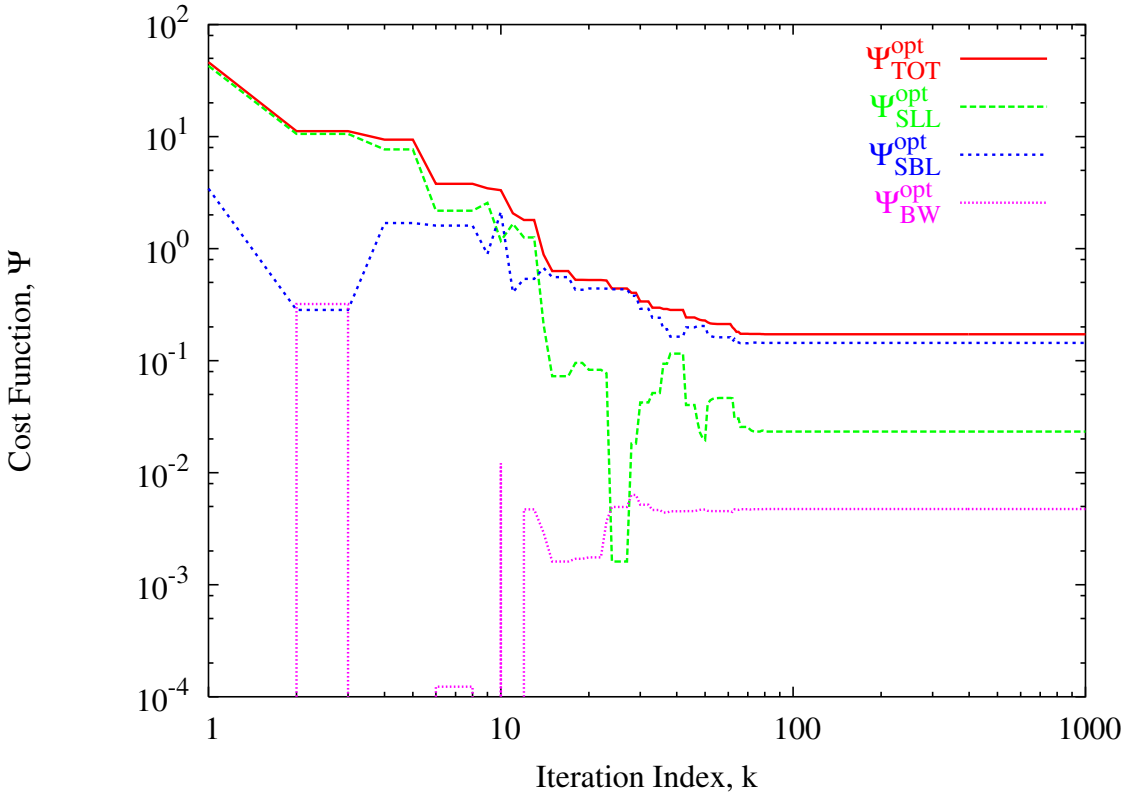

Fig. 14 - L. Poli *et al.*, "Pattern synthesis in time-modulated linear arrays ..."